JOC The Journal of Organic Chemistry

Article

pubs.acs.org/joc

Vinylnitrene Formation from 3,5-Diphenyl-isoxazole and 3-Benzoyl-2-phenylazirine

Disnani W. Gamage, Qian Li, R. A. A. Upul Ranaweera, Sujan K. Sarkar, Geethika K. Weragoda, Patrick L. Carr, and Anna D. Gudmundsdottir*

Department of Chemistry, University of Cincinnati, Cincinnati Ohio 45221-0172, United States

Supporting Information

ABSTRACT: Photolysis of **1** in argon-saturated acetonitrile yields **2**, whereas in oxygen-saturated acetonitrile small amounts of benzoic acid and benzamide are formed in addition to **2**. Similarly, photolysis of **2** in argon-saturated acetonitrile results in **1** and a trace amount of **3**, whereas in oxygen-saturated acetonitrile the major product is **1** in addition to the formation of small amounts of benzoic acid and benzamide. Laser flash photolysis of **1** results in an absorption due to triplet vinylnitrene **4** (broad absorption with λ_{max} at 360 nm, τ = 1.8 μs, acetonitrile) that is formed with a rate constant of 1.2×10^7 s^{-1} and decays with a rate constant of 5.6×10^5 s^{-1}. Laser flash photolysis of **2** in argon-saturated acetonitrile likewise results in the formation of triplet vinylnitrene **4** but also ylide **5** (λ_{max} at 440 nm, τ = 13 μs). The rate constant for forming **4** in argon-saturated acetonitrile is 1.6×10^7 s^{-1}. In oxygen-saturated acetonitrile, vinylnitrene **4** reacts to form the peroxide radical **6** (λ_{max} 360 nm, ~0.7 μs, acetonitrile) at a rate of 2×10^9 M^{-1} s^{-1}. Density functional theory calculations were performed to aid in the characterization of vinylnitrene **4** and peroxide **6** and to support the proposed mechanism for the formation of these intermediates.

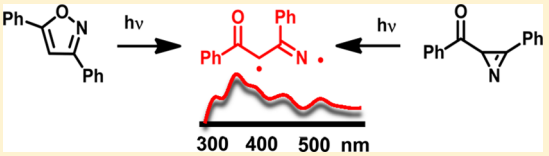

1. INTRODUCTION

Nitrenes are monovalent electron-deficient intermediates that have either a triplet or singlet configuration.[1−6] Singlet nitrenes are generally highly reactive, short-lived intermediates that primarily decay by unimolecular rearrangement. However, some of the more stable singlet nitrenes are sufficiently long-lived to undergo bimolecular reactions, and because they can efficiently insert into neighboring molecules, they have been used in various applications, such as surface modification,[7] cross-polymerization[8] and photoaffinity labeling.[9] In comparison, triplet nitrenes are generally less reactive and are thus longer-lived intermediates because they require intersystem crossing to form products. Due to their high spin properties, triplet nitrenes have the potential to be building blocks for high-spin assemblies.[10] It is not only the spin state of nitrenes that affects their reactivity. In addition, electron-donating substituents, such as aryl- and alkyl groups, stabilize the nitrene intermediates further, whereas electron-withdrawing substituents destabilize nitrenes. For example, triplet aryl- and alkylnitrenes are long-lived intermediates with lifetimes on the order of milliseconds because they do not react with the solvent but rather decay by dimerization.[11−14] The measured rate at which triplet alkylnitrenes react with molecular oxygen is ~5×10^4 M^{-1} s^{-1},[11] and the rate for trapping triplet phenylnitrenes with oxygen has been determined to be between 5×10^4 and 8×10^6 M^{-1} s^{-1},[15−17] which is considerably slower than diffusion, i.e., the rate at which most C-centered radicals react with oxygen.

Recently, we reported the first direct detection of a triplet vinylnitrene in solution by performing laser flash photolysis of (3-methyl-2*H*-azirin-2-yl)phenylmethanone (Scheme 1).[18]

Scheme 1

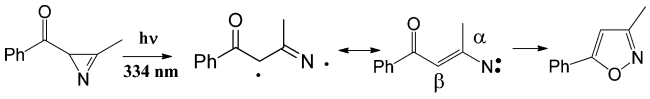

Triplet Vinylnitrene

Although this triplet vinylnitrene has an electron-donating vinyl substituent, it has a lifetime of only a few microseconds in solution and is efficiently quenched with molecular oxygen at a rate of 7×10^8 M^{-1} s^{-1}.[18] Spin density calculations show that the triplet vinylnitrene has significant 1,3 biradical character with substantial spin density on the β C-atom, which explains why this vinylnitrene reacts efficiently with molecular oxygen at rates that are comparable to those generally observed for C-atom centered radicals. We were, however, not able to isolate any photoproducts that result from trapping the triplet vinylnitrene with oxygen, whereas Murata et al. have previously reported that the vinylnitrene depicted in Scheme 2 can be trapped with molecular oxygen to form stable compounds.[19]

Scheme 2

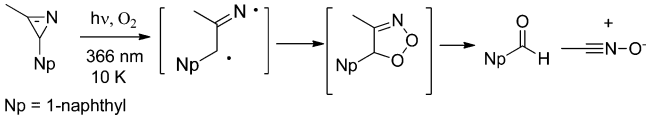

Np = 1-naphthyl

Received: August 29, 2013
Published: October 15, 2013

   dx.doi.org/10.1021/jo401819g | J. Org. Chem. 2013, 78, 11349−11356

In this study, we used laser flash photolysis to demonstrate that both isoxazole **1** and azirine **2** can serve as precursors for triplet vinylnitrene **4**. As expected, vinylnitrene **4** is short-lived and decays by intersystem crossing to reform **1** and **2**. In oxygen-saturated acetonitrile, triplet vinylnitrene **4** is intercepted by oxygen to form peroxide radical **6**, which can be observed directly with laser flash photolysis. The rate for the reaction of vinylnitrene **4** with oxygen was estimated to be 2.1×10^9 M^{-1} s^{-1}. Thus, in this paper, we have further demonstrated that triplet vinylnitrenes show 1,3-biradical character, which is shown by their efficient reactivity with molecular oxygen.

2. RESULTS

2.1. Product Studies. Irradiation of **1** in argon-saturated $CDCl_3$, through a Pyrex filter, resulted in the formation of **2** as the only photoproduct (Scheme 3), whereas photolysis of **2**

Scheme 3. Photolysis of 1 in Argon- and Oxygen-Saturated $CDCl_3$

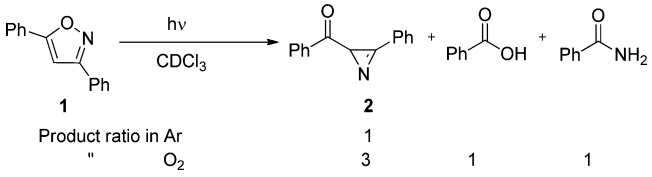

through a Pyrex filter in argon-saturated $CDCl_3$ forms **1** and a trace amount of **3** at 55% conversion (Scheme 4). The results agree with those previously reported by Singh et al.[20]

In comparison, irradiation of **1** in oxygen-saturated $CDCl_3$, through a Pyrex filter, also resulted in formation of **2**, benzoic acid and benzamide in a ratio of 3:1:1 with 37% conversion (Scheme 3). Similarly, photolysis of **2** in oxygen-saturated $CDCl_3$ results in formation of **1**, benzoic acid, benzamide in the ratio 8:1:1 as well as a trace amount of **3** with 54% conversion (Scheme 4).

Thus, we theorize that upon irradiation, both **1** and **2** form triplet excited states, which undergo C−N bond cleavage to form triplet vinylnitrene **4** (Scheme 5). Triplet vinylnitrene **4** must decay by intersystem crossing and reforms both **1** and **2** in argon-saturated $CDCl_3$, whereas in oxygen-saturated $CDCl_3$, vinylnitrene **4** is intercepted by oxygen to form benzoic acid and benzamide (Scheme 6).

Singh et al. proposed that **3** is formed by cleavage of the C−C bond of the azirine moiety in **2** to form ylide **5** (Scheme 7).[20] There are several examples in the literature demonstrating that the photolysis of azirine derivatives yields ylides such as **5**[21−25] and that these reactions proceed on the singlet surface of the azirine.[26] Thus, azirine **2** is a precursor to triplet vinylnitrene **4**, but **2** also undergoes singlet reactivity to form **3**.

2.2. Calculations. To better compare the photoreactivities of **1** and **2**, we calculated stationary points on the singlet and

Scheme 5. Proposed Mechanism for the Reaction of 1 and 2 on Their Triplet Energy Surface

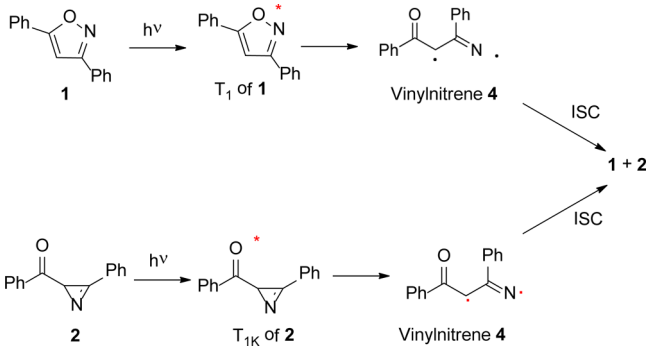

Scheme 6. Proposed Mechanism for Trapping Vinylnitrene 4 with Oxygen

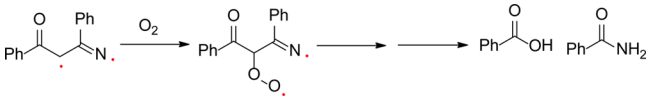

Scheme 7. Proposed Mechanism Showing the Singlet Photoreactivity of 2

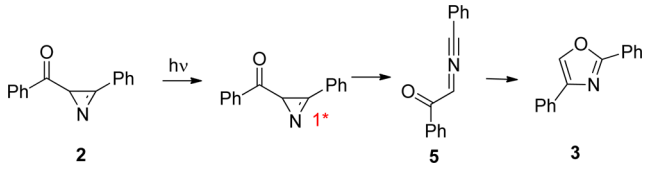

triplet surfaces of **1** and **2** using the B3LYP level of theory with the 6-31G+(d) basis as implemented on Gaussian09.[27−29]

We compared the triplet excited states of **1** and **2**. Time-dependent density functional theory (TD-DFT) calculations located the first excited singlet state (S_1) of **1** at 103 kcal/mol above the S_0 of **1**, whereas the first and second excited triplet state (T_1, T_2) of **1** were located 65 and 76 kcal/mol above the S_0 of **1** (Figure 5), respectively.

We also optimized the T_1 of **1** and found that it is located 63 kcal/mol above the S_0. The energies for the T_1 of **1** obtained from TD-DFT and optimization calculations are in good agreement, presumably because the geometries of T_1 and S_0 of **1** are fairly similar and therefore the vertical excitation and equilibrium energies are comparable. In the optimized structure of the T_1 of **1**, the O−C and the N−C bonds are 1.42 and 1.42 Å and are thus somewhat longer than the corresponding bonds in the S_0 of **1**, which are 1.36 and 1.32 Å, respectively. In addition, the C═C bonds in the phenyl ring adjacent to the oxygen atom in the T_1 of **1** are no longer equivalent, as in the S_0 of **1**. Thus, T_1 is best described as a triplet excited state that is delocalized throughout the isoxazole moiety and the phenyl group adjacent to the oxygen atom. Spin density calculations

Scheme 4. Photolysis of 2 in Argon- and Oxygen-Saturated $CDCl_3$

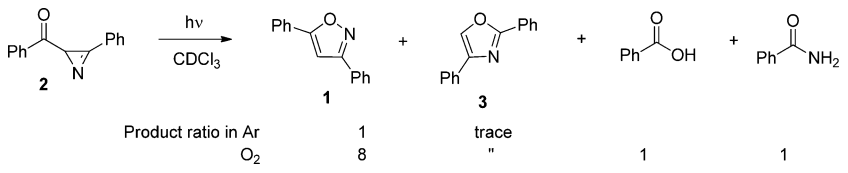

dx.doi.org/10.1021/jo401819g | J. Org. Chem. 2013, 78, 11349−11356

further support this notion, as they show that the unpaired spin is mainly localized on the isoxazole moiety and the phenyl group adjacent to the oxygen atom (Figure 1, Scheme 8).

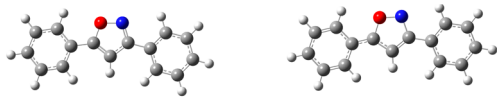

Bond	(Å)	(Å)
C-O	1.36	1.42
C=N	1.32	1.42
O-N	1.39	1.39
NC-Ph	1.48	1.46
OC-CPh	1.46	1.39
OC-CH	1.37	1.43
NC-CH	1.43	1.37

Figure 1. Selected bond distances (Å) in the optimized structure of **1** and the T_1 of **1**.

TD-DFT calculations of the optimized structure of **2** place the first and second excited triplet state of the ketone (T_{1K} and T_{2K}) of **2** at 68 and 73 kcal/mol, respectively, above its S_0, or 82 and 87 kcal/mol with respect to the S_0 of **1** (Figure 5). Inspection of the molecular orbitals indicates that the T_{1K} of **2** has an (n,π^*) configuration, whereas the T_{2K} of **2** has a (π,π^*) configuration.

The optimized structure of the T_{1K} of **2** is located 65 kcal/mol above the S_0. The progression of the C═O bond in the T_{1K} of **2** to 1.31 Å from 1.23 Å in the S_0 of **2** indicates that this triplet state has an (n,π^*) configuration, which is in an agreement with the TD-DFT calculations. The energy obtained for the optimized structure of the T_{1K} of **2** is only slightly less than the energy obtained from the TD-DFT calculations, although the geometries of T_{1K} and S_0 of **2** are different, thus indicating that the potential energy surface of T_{1K} of **2** must be relatively flat. We have, however, previously shown that B3LYP calculations underestimate the energy of triplet ketones with an (n,π^*) configuration.[30] Spin density calculations further support this because the spin density is primarily localized on the oxygen atom in the C═O moiety and the adjacent phenyl ring (Scheme 8).

We also optimized the structure of the T_A of **2** and found that the energy level is located 63 kcal/mol above the S_0 of **2**. In the T_A of **2**, the C═O bond is 1.22 Å, which is similar to the C═O bond in the S_0 of **2**, 1.23 Å (Figure 2), whereas the C−C bond in the azirine ring is shorter than in the S_0 of **2**. Furthermore, the C═N bond in the T_A of **2** progressed to 1.42 Å compared to 1.26 Å in the S_0 of **2**, whereas the C−C bond in the azirine ring is condensed to 1.37 Å in the T_A of **2** compared to 1.45 Å in the S_0 of **2**. The calculated spin density of the T_A of **2** is shown in Scheme 8, which shows that the unpaired electrons are mainly localized on the azirine ring and the adjacent phenyl ring. Thus, the calculations show that the T_A of **2** is localized on the azirine moiety and the phenyl group that is conjugated with the azirine (Figure 2).

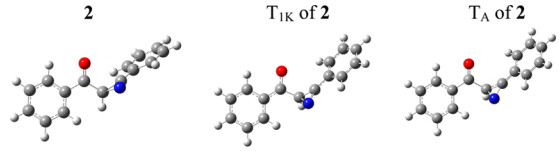

Bond	(Å)	(Å)	(Å)
C=O	1.23	1.32	1.22
C=N	1.26	1.27	1.43
C=O-CH	1.50	1.49	1.55
Ph-C=O	1.50	1.42	1.49
Ph-C=N	1.45	1.45	1.37
CH-CPh	1.47	1.46	1.43

Figure 2. Selected bond distances (Å) in the optimized structure of **2** and T_{1K} of **2** and T_A of **2**.

Two minimal energy conformers were calculated for triplet vinylnitrene **4**, **A** and **B**, and **A** was slightly more stable, by ∼0.7 kcal/mol (Figure 3). The calculated spin density of **4** demonstrates that the triplet vinylnitrene **4** has considerable 1,3-carbon iminyl biradical character, as the spin density is mainly located on the N and the β-C atoms (Scheme 8). The biradical character of vinylnitrene **4** can be further highlighted by calculating the rotational barrier between conformer **4A** and **4B**, which is ∼7.5 kcal/mol and thus significantly lower than for a simple C═C bond (Figure 4).

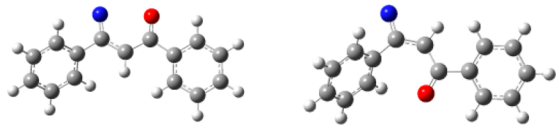

Bond	(Å)
C=O	1.23
CO-CH	1.47
CH-CN	1.43
C=N	1.30

Figure 3. Relative energy of the minimal energy conformers A and B of vinylnitrene **4** and selected bond lengths (Å).

The stationary points on the triplet surface of **1** and **2**, relative to S_0 of **1**, to form vinylnitrene **4** are shown in Figure 5. The calculations show that vinylnitrene **4** can be formed from both the T_{1K} of **2** and the T_1 of **1**, but the transition state barrier for forming vinylnitrene **4** is considerably larger for the T_1 of **1** than for the T_{1K} of **2**. However, it is possible that vinylnitrene **4** is formed from the T_2 of **1**. Direct irradiation of the S_1 of **1** can result in intersystem crossing to the T_2 of **1** rather than to the T_1 of **1** because the S_1 and T_2 of **1** are closer in energy.

The transition state energy for forming ylide **5** was calculated to be 44 kcal/mol above the S_0 of **2**. IRC calculations correlate this transition state with the S_0 of **2** and ylide **5** (Figure 6).

Scheme 8. Calculated Spin Densities for the T_1 of 1, T_{1K} of 2, T_A of 2 and 4

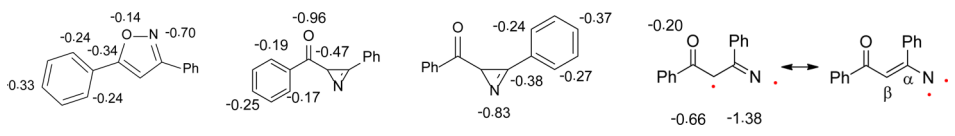

dx.doi.org/10.1021/jo401819g | J. Org. Chem. 2013, 78, 11349−11356

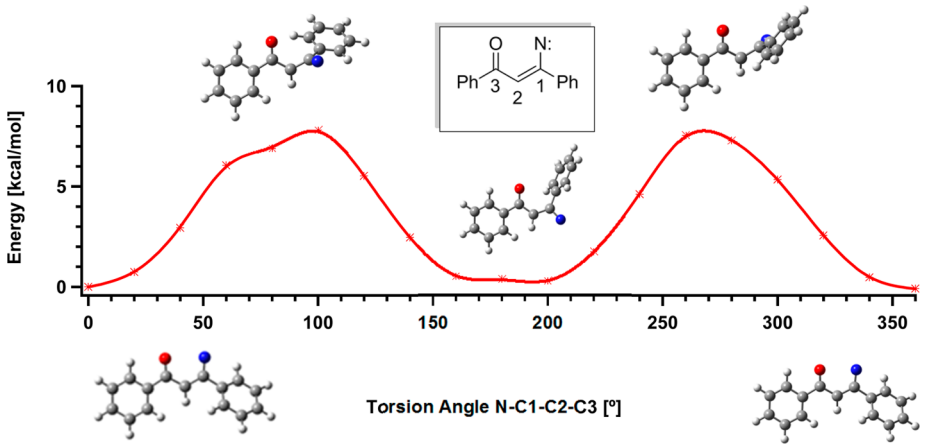

Figure 4. Calculated rotational barriers between vinylnitrene conformers **4A** and **4B**.

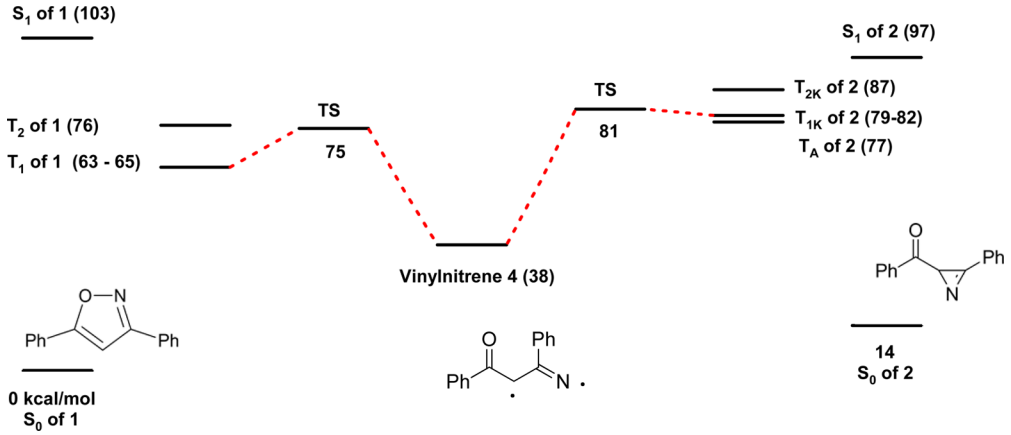

Figure 5. Calculated stationary points for the triplet surface of **1** and **2**. The calculated energies are in kcal/mol and are relative to S_0 of **1**. The energies of the S_1 and T_2, T_1 (65) of **1**, S_1, T_{2K} and T_{1K} (82) of **2** were obtained from the TD-DFT calculations, whereas the energies of the transition states (TS) and the S_0 and T_1 (63) of **1** and the S_0, T_{1K} (79), and T_A of **2** were obtained by optimization.

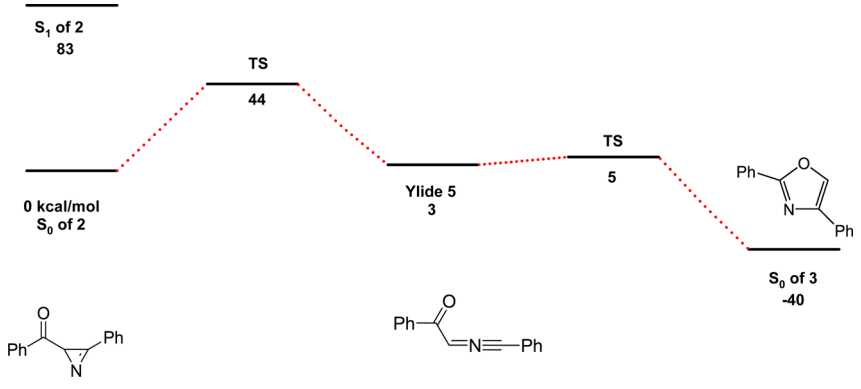

Figure 6. Calculated stationary points for the singlet surface of **2**. The calculated energies are in kcal/mol. The energy of the S_1 of **2** was obtained by TD-DFT calculations, whereas the energies of the transition states (TS) S_0 of **2** and S_0 of **2** and **3** were obtained by optimization.

We also explored the reactivity of vinylnitrene **4** with oxygen to form radicals **6** and **7** (Figure 7). The calculated triplet transition state for the addition of oxygen to **4** to form **6** is located 6 kcal/mol above **4** and that of an oxygen molecule. Radical **6** is 7 kcal/mol more stable than vinylnitrene **4** and oxygen. In comparison, the transition state to form **7** is located 16 kcal/mol above **4**, and that of an oxygen molecule and radical **7** is 5 kcal/mol less stable than **4** and an oxygen molecule. Thus, the calculations show that intercepting vinylnitrene **4** with oxygen to form **6** is feasible at ambient temperature and that the formation of **6** is strongly favored over **7** (Figure 7).

2.3. Phosphorescence. The phosphorescence spectra of **1** and **2** were obtained on a phosphorometer in frozen ethanol matrices at 77 K (Figure 8). Because the emission from **1** and **2** is not sufficiently resolved to locate the (0,0) transitions, we used the onset of the emission at the shortest wavelength to estimate the (0,0) transitions for the T_1 of **1** and T_{1K} of **2**. The estimated onset for phosphorescence for **1** is 471 nm, which corresponds to the T_1 of **1** being 61 kcal/mol above the S_0 of **1**

dx.doi.org/10.1021/jo401819g | J. Org. Chem. 2013, 78, 11349−11356

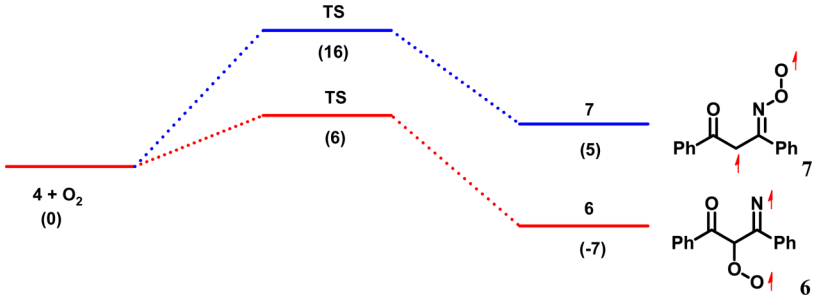

Figure 7. Energy diagram for forming triplet peroxide radicals **6** and **7**. (Energies are in kcal/mol.)

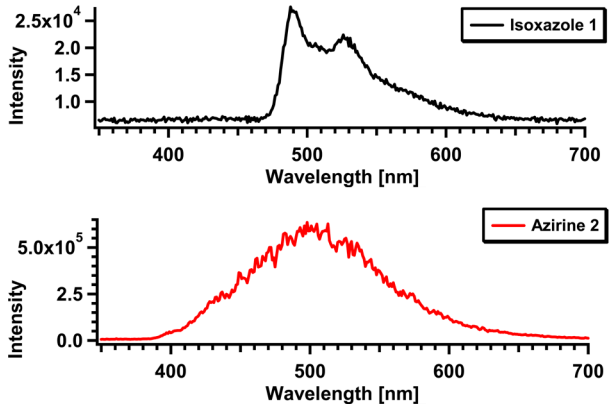

Figure 8. Phosphorescence spectra of **1** and **2** in ethanol glasses at 77 K obtained with excitation at 340 nm.

(Table 1). In comparison, the estimated onset of phosphorescence of **2** is observed at ~400 nm; thus, the T_{1K} of **2** is ~71

Table 1. Energies of the T_1 of 1 and the T_{1K} of 2

	phosphorescence			
cmpd	wavelength (nm)	energy (kcal/mol)	TD-DFT[a]	optimized[b]
T_1 of **1**	471	61	65	63
T_{1K} of **2**	400	71	68	65

[a]The energies were obtained from TD-DFT (B3LYP/6-31G+(d)) calculations. [b]The energies were obtained from optimization (B3LYP/6-31G+(d)) calculations.

kcal/mol above the S_0 of **2**. The calculated and measured energies for the T_1 of **1** and the T_{1K} of **2** are in good agreement (Table 1).

2.4. Laser Flash Photolysis. To directly identify vinylnitrene **4** and its triplet precursors, we performed laser flash photolysis of **1** and **2** (308 nm[31]). Laser flash photolysis of **1** in argon-saturated acetonitrile or methanol resulted in a broad absorption with a λ_{max} of ~360 nm that trails off to 550 nm (Figure 9). The calculated spectrum of the T_1 of **1** in acetonitrile has major electronic transitions at 531 (f = 0.147), 512 (f = 0.104), 453 (f = 0.074), 392 (f = 0.057), and 333 (f = 0.31) nm (Figure 10), which agrees with the observed spectrum. Likewise, the calculated spectra of **4A** and **4B** in acetonitrile have major electronic transitions at 344 (f = 0.043), 347 (f = 0.024), 525 (f = 0.029), and 540 (f = 0.036) nm, which also agree with the observed spectra, even though the absorption is not as intense at longer wavelengths as the calculations predict. To further aid in the assignment of this transient absorption, we performed laser flash photolysis of **1** in

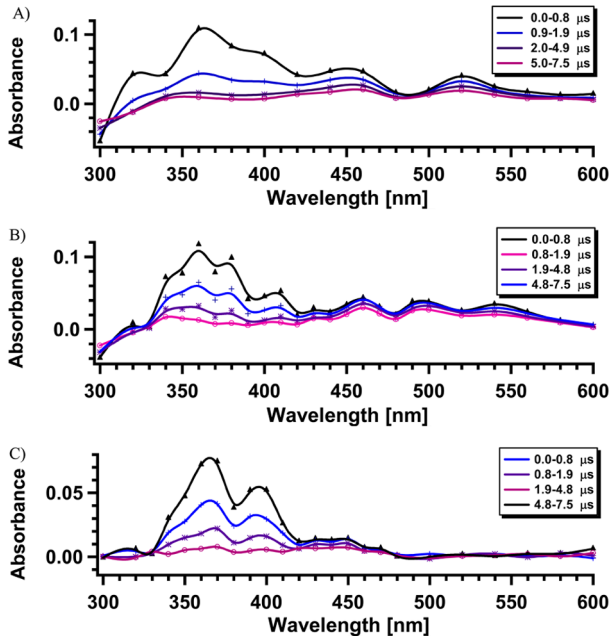

Figure 9. Transient spectra obtained from laser flash photolysis of **1** in (A) argon-saturated acetonitrile and (B) argon-saturated and (C) oxygen-saturated methanol.

oxygen-saturated methanol and acetonitrile, and this resulted in a broad transient spectrum with a λ_{max} at 360 nm. This transient spectrum does show absorption above 480 nm and therefore does not correlate to either the T_1 of **1** or vinylnitrene **4**. Thus, we theorized that in oxygen-saturated solution the transient absorption results from the reaction of vinylnitrene **4** with oxygen to form peroxyradical **6**, because the observed spectrum matches the calculated spectrum of **6** (Figures 9C and 10C).

Kinetic studies further support the assignments of the transient spectra obtained from the laser flash photolysis of **1**. At 360 nm, the absorption is formed with a rate constant of 1.2×10^7 s^{-1} (τ = 83 ns) in argon-saturated acetonitrile, whereas the decay of the transient absorption is best fitted as an exponential function, which yields a decay rate constant of 5.5×10^5 s^{-1}. Thus, vinylnitrene **4** is formed at a rate of 1.2×10^7 s^{-1} from its precursor and has a lifetime of 1.8 μs. It should be highlighted that the transient absorption at 460 nm forms and decays with the same rate constants as the absorption at 360 nm in argon-saturated solution. In oxygen-saturated acetonitrile (Figure 11), the transient absorption is formed at a rate of 1.65×10^7 s^{-1} (τ = 61 ns) and it decays at a rate of 1.35×10^6 s^{-1} (τ = 743 ns). Furthermore, the absorption intensity is higher at 360 nm in oxygen-saturated solution compared to argon-saturated solution. Kinetic analysis at 460 nm shows that in

dx.doi.org/10.1021/jo401819g | J. Org. Chem. 2013, 78, 11349−11356

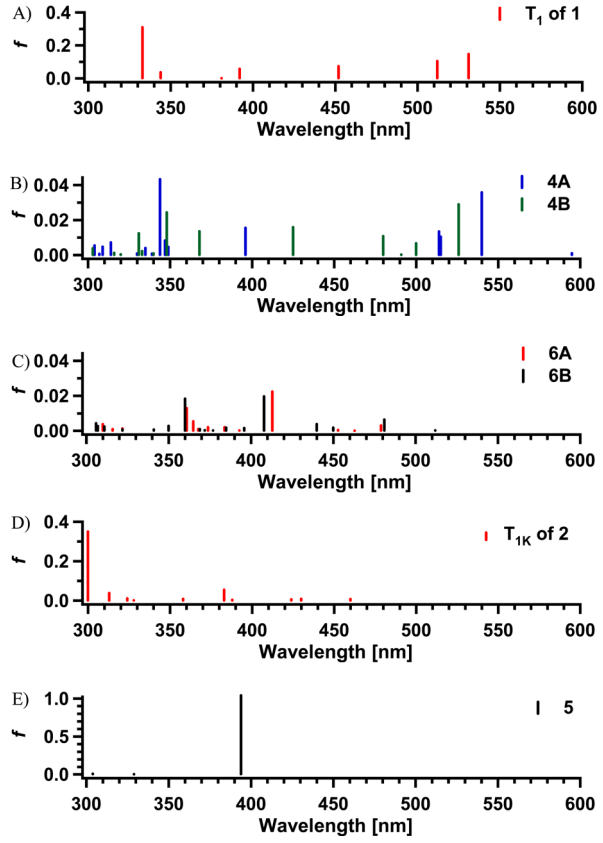

Figure 10. Calculated electronic transitions in acetonitrile for T_1 of (A) **1**, (B) **4A** and **4B**, (C) **6A** and **6B**; T_K of (D) **2** and (E) ylide **5**.

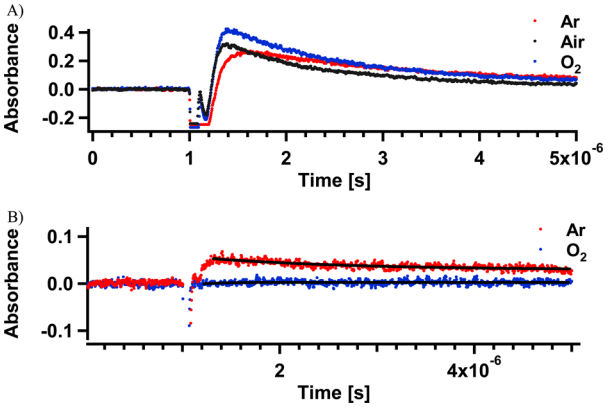

Figure 11. Kinetic traces obtained at (A) 360 nm and (B) 460 nm for the laser flash photolysis of **1** in argon-, air- and oxygen-saturated acetonitrile.

oxygen-saturated solution, the absorption is quenched and not enhanced, as it is at 360 nm, thus further supporting that a different transient is formed in oxygen-saturated solutions compared to argon-saturated solutions. Therefore, we conclude that triplet vinylnitrene **4** reacts with oxygen with a rate constant of 1.65×10^7 s^{-1}, and because the concentration of oxygen in saturated acetonitrile is 0.009 M,[32−34] the rate for oxygen quenching of vinylnitrene **4** is 1.8×10^9 $M^{-1}s^{-1}$, which is similar to what we have previously measured for another vinylnitrene derivative.[35]

The laser flash photolysis of **2** in argon-saturated acetonitrile produced a transient spectrum showing a broad absorption with the λ_{max} at 360 nm (Figure 12). We assign this absorption to

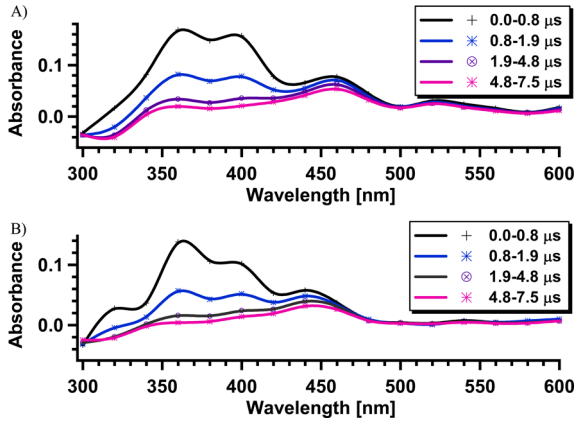

Figure 12. Transient spectra obtained from laser flash photolysis of **2** in (A) argon-saturated and (B) oxygen-saturated acetonitrile.

vinylnitrene **4** and ylide **5** based on the following. The observed transient spectra was similar to the one obtained from the laser flash photolysis of **1** in argon-saturated solution, thus supporting the theory that transient absorption is due to vinylnitrene **4**. Furthermore, the calculated absorption spectrum of the T_K of **2** does not match the observed spectra. In oxygen-saturated acetonitrile, laser flash photolysis of **2** resulted in a transient spectrum that is similar to the one obtained by laser flash photolysis of **1** in oxygen-saturated acetonitrile, but there is an additional absorption band at 440 nm that we assign to ylide **5** in addition to the absorption due to formation of peroxide radical **6**. The major calculated transition for ylide **5** is located at 394 nm (f = 1.04), which fits reasonably with the band observed at 440 nm.

As before, kinetic analysis further supported these absorption assignments (Figure S1 in the Supporting Information [SI]). The absorption of vinylnitrene **4** at 360 nm is formed with a rate constant of 2.0×10^7 s^{-1} (τ = 50 ns), and it decays with a rate constant of 6.0×10^5 s^{-1} (τ = 1.7 μs) in argon-saturated acetonitrile. As expected, vinylnitrene **4** is formed with a different rate constant from the excited states of **1** and **2**, whereas the lifetime of vinylnitrene **4** is the same, within experimental error. The transient absorption at 440 nm can be fitted as biexponential decay with rate constants of 6.5×10^5 s^{-1} (τ = 1.5 μs) and 7.68×10^5 s^{-1} (τ = 13 μs), with the shorter-lived component corresponding to vinylnitrene **4** and the longer-lived component to ylide **5**. Ylide **5** has a lifetime similar to those of other ylides that decay by intramolecular reaction, but it is much shorter lived than those of ylides that decay by bimolecular reactions.[18,36] The transient absorption at 500 nm forms and decays with the same rate constants as the absorption at 360 nm.

In addition, kinetic analysis in oxygen-saturated acetonitrile shows that the transient absorption at 360 nm is formed with a rate constant of 1.63×10^7 s^{-1} (τ = 61 ns) and decays with a rate constant of 1.40×10^6 s^{-1} (τ = 714 ns), which fits nicely with the rate constants measured from the reactivity of **1**. Analysis of the transient kinetics at 500 nm shows that, in oxygen-saturated solution, the absorption is fully quenched.

3. DISCUSSION

Laser flash photolysis has demonstrated that both **1** and **2** yield vinylnitrene **4**. Although the calculated transition state barrier for forming vinylnitrene **4** from the T_1 of **1** is considerably higher than that for the T_{1K} of **2**, the rate of forming

dx.doi.org/10.1021/jo401819g | J. Org. Chem. 2013, 78, 11349−11356

vinylnitrene **4** from these two compounds is on the same order. Thus, we theorize that the S_1 of **1** does not intersystem cross to the T_1 of **1** but rather to a higher-lying triplet excited state that is closer in energy to the S_1 of **1** and then cleaves to form vinylnitrene **4**. Thus, both isoxazole and azirine are effective precursors for forming triplet vinylnitrene intermediate **4**. Azirine **2** is, however, somewhat less selective than **1** because excitation of the azirine chromophore in **2** leads to formation of ylide **5**, whereas excitation of the ketone chromophore in **2** yields the S_{1K} of **2** that will intersystem cross to form the T_{1K} of **2**. The conjugation of the phenyl ring with the azirine moiety lowers the triplet energy of the T_A of **2** significantly, and its triplet energy is comparable to the T_{1K} of **2**. However, the TD-DFT calculations of the S_0 of **2** show that the main absorption above 300 nm is due to the ketone chromophore; thus, the main reactivity observed is the formation of triplet vinylnitrene **4**. Furthermore, 3-phenyl-2H-azirine (**8**) has been shown to undergo singlet reactivity upon direct irradiation; thus, it is not likely that the singlet excited state of the azirine moiety in **2** intersystem crosses to form the T_A of **2** (Scheme 9).[36]

Scheme 9

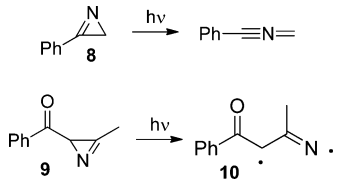

The transient spectrum of vinylnitrene **4** is somewhat similar to the transient spectrum of vinylnitrene **10** (Scheme 9); they both have broad absorptions with a λ_{max} at 360 nm that trail out to 500 nm.[18] The absorption in vinylnitrenes **4** and **10** are due to several electronic transitions between the lone pair on the oxygen, the half-filled p-orbital on the N-atom and the π-orbitals into the half-filled p-orbital on the N-atom, and the π^*-orbitals. Vinylnitrenes **4** and **10** also have similar lifetimes of a few microseconds because they both decay by efficient intersystem crossing to their singlet states. Presumably, the intersystem crossing is efficient because the triplet vinylnitrenes intersystem cross to their singlet vinylnitrenes, which have open shell configurations.[37,38]

The calculated spin densities of vinylnitrenes **4** and **10** are similar. The spin density is mainly located on the N-atom and the β-C atom; thus, the increased conjugation of the vinylnitrene chromophore to the additional phenyl group in **4** does not affect the spin density. The most significant difference between triplet vinylnitrenes **4** and **10** is that vinylnitrene **4** reacts with oxygen to form stable products, benzoic acid and benzamide, whereas **10** did not yield any new products in oxygen-saturated solutions (Scheme 9). It can be theorized that in oxygen-saturated solution, the triplet ketone in **9** is efficiently quenched; thus, no new products were observed from attempts to trap the vinylnitrene **10** with oxygen, or the products were not stable enough to be isolated. More importantly, it was possible to detect the peroxide radical **6** directly by performing laser flash photolysis of **1** and **2** in oxygen-saturated acetonitrile, thereby experimentally verifying that vinylnitrene **4** has significant 1,3-biradical character, as oxygen adds to the β-C atom. In addition, the TD-DFT calculations demonstrate that the intensities of the calculated electronic transitions for vinylnitrene **4** are more significant than those for **10** due to the involvement of the additional phenyl chromophore. The rates of vinylnitrenes **4** and **10** when reacting with oxygen are efficient, 7×10^8 and 2×10^9 $M^{-1}s^{-1}$, respectively, because the oxygen adds to the β-carbon atom in the vinylnitrenes and not the nitrogen atom, as in triplet alkyl- and phenylnitrenes.

4. CONCLUSION

We have shown that azirine **2** and isoxazole **1** can both serve as precursors to triplet vinylnitrene **4**, which is a short-lived intermediate. Spin density calculations show that triplet vinylnitrene **4** has significant spin density on the β-carbon atom, thus demonstrating that vinylnitrene **4** has significant 1,3-biradical character. Therefore, it reacts efficiently with oxygen to form peroxide radical **6**.

EXPERIMENTAL SECTION

Calculation. All the geometries were optimized at the B3LYP level of theory and with the 6-31G+(d) basis set as implemented in the Gaussian03/09 programs.[28,29,39] All transition states were confirmed to have one imaginary vibrational frequency by analytical determination of the second derivatives of the energy with respect to internal coordinates. Intrinsic reaction coordinate (IRC) calculations were used to verify that the optimized transition states corresponded to the attributed reactant and product.[40,41] The absorption spectra were calculated using time-dependent density functional theory (TD-DFT).[42−45] The effect of solvation was calculated using the self-consistent reaction field (SCRF) method with the integral equation formalism polarization continuum model (IEFPCM) with acetonitrile as the solvent.[46−49] All calculations were performed at the Ohio Supercomputer Center.

Laser Flash Photolysis. Laser flash photolysis was performed with an Excimer laser (308 nm, 17 ns).[31] A stock solution of **1** or **2** in acetonitrile or methanol was prepared with spectroscopic-grade acetonitrile or methanol, so that the solutions had absorption between 0.6 and 0.4 at 308 nm. Typically, 3 mL of the stock solution was placed in a 10 mm × 10 mm wide, 48 mm long quartz cuvette and it was purged with argon or oxygen for 5 min. The rates were obtained by fitting an average of three kinetic traces. Transient absorption spectra were obtained by plotting average absorbance values collected from decays at 10 or 20 nm intervals between 300 and 600 nm.

Preparation of 1. Dibenzoylmethane (2.24 g, 10 mmol) and $NH_2OH{\cdot}HCl$ (0.725 g, 10.5 mmol) in absolute ethanol (25 mL) were refluxed for 3 h. The mixture was cooled and diluted with water until 3,5-diphenyl isoxazole precipitated. The precipitate was washed with water and dried in a vacuum desiccator and recrystallized from diethyl ether. The ^{1}H NMR spectrum of **1** was identical to that previously reported.[50] ^{1}H NMR (400 MHz, $CDCl_3$): δ 7.84−7.89 (m, 4H), 7.46−7.51 (m, 6H), 6.84 (s, 1H) ppm. GC−MS m/z (EI) 221 (M^+, 30), 193, 165, 144, 116, 105 (100), 89, 77, 63, 51. IR (neat, ν_{max}): 3114, 1489, 1457, 1046, 951, 914, 820, 763, 689 cm^{-1}.

Preparation of 2. 3,5-Dibenzoyl isoxazole (500 mg, 2.2 mmol) in argon-saturated $CHCl_3$ was irradiated through a Pyrex filter until GC−MS analysis of the reaction mixture showed 30% formation of **2** (30 mg, 0.14 mmol, 6% yields) and 70% of remaining starting material. Azirine **2** was separated from the starting material using a silica column eluted with 5% ethyl acetate in hexane. The ^{1}H NMR spectrum of **2** matches the one reported in the literature.[50] ^{1}H NMR (400 MHz, $CDCl_3$): δ 8.13−8.15 (d, J = 8 Hz, 2H), 7.87−7.89 (d, J = 8 Hz, 2H), 7.61−7.66 (m, 2H), 7.53−7.58 (m, 4H), 3.86 (s, 1H) ppm. GC−MS. (EI) m/z: 221 (M^+, 30), 193, 165, 144, 116, 105 (100), 89, 77 (66), 63, 51. IR (neat, ν_{max}): 3062, 1775, 1672, 1597, 1579, 1449, 1351, 1230, 1009, 721, 688, 653 cm^{-1}.

Photolysis of 1. A solution of **1** (75 mg, 0.33 mmol) in argon-saturated $CDCl_3$ was irradiated through a Pyrex filter for a day using a medium-pressure mercury arc lamp. ^{1}H NMR spectrum of the reaction mixture showed the formation of **2** and remaining starting material in the ratio of 1:2.

dx.doi.org/10.1021/jo401819g | J. Org. Chem. 2013, 78, 11349−11356

A solution of **1** (75 mg, 0.33 mmol) in oxygen-saturated $CDCl_3$ were irradiated through a Pyrex filter for a day using a medium-pressure mercury arc lamp. ^1H NMR spectroscopy and GC–MS analysis of the reaction mixture showed the formation of **2**, benzoic acid and benzamide in the ratio of 4:1:1 at 40% conversion.

Photolysis of 2. A solutions of **2** (30 mg, 0.13 mmol) in argon-saturated $CDCl_3$ was irradiated through a Pyrex filter for 24 h using a medium-pressure mercury arc lamp. ^1H NMR spectrum of the reaction mixture showed the formation of **1** and remaining **2**, along with trace amounts of **3**, at 45% conversion.

A solutions of **2** (30 mg, 0.13 mmol) in oxygen-saturated $CDCl_3$ was irradiated through a Pyrex filter (>300 nm) for 24 h using a medium-pressure mercury arc lamp. ^1H NMR spectroscopy and GC–MS analysis of the reaction mixture showed the formation of **1**, benzoic acid, and benzamide in the ratio of 8:1:1, respectively, along with trace amount of **3** at 55% conversion.

■ ASSOCIATED CONTENT

Supporting Information

Cartesian coordinates and energies of **1**–**7** and NMR spectra of **1** and **2**. This material is available free of charge via the Internet at http://pubs.acs.org.

■ AUTHOR INFORMATION

Corresponding Author

*Anna.Gudmundsdottir@uc.edu

Notes

The authors declare no competing financial interest.

■ ACKNOWLEDGMENTS

We thank the National Science Foundation (CHE-1057481) and the Ohio Supercomputer Center for supporting this work.

■ REFERENCES

(1) Platz, M. S. In *Reactive Intermediate Chemistry*; John Wiley & Sons, Inc.: 2005, p 501.
(2) Gritsan, N. P.; Platz, M. S.; Borden, W. T. *Mol. Supramol. Photochem.* **2005**, *13*, 235.
(3) Gritsan, N. P.; Platz, M. S. *Chem. Rev.* **2006**, *106*, 3844.
(4) Platz, M. S. *Nitrenes*; John Wiley & Sons, Inc., 2004.
(5) Bucher, G., Ed. *Photochemical Reactivity of Azides*; CRC Press: Boca Raton, 2004.
(6) Platz, M. S. *Acc. Chem. Res.* **1995**, *28*, 487.
(7) Mecomber, J. S.; Murthy, R. S.; Rajam, S.; Singh, P. N. D.; Gudmundsdottir, A. D.; Limbach, P. A. *Langmuir* **2008**, *24*, 3645.
(8) Jadhav, A. V.; Gulgas, C. G.; Gudmundsdottir, A. D. *Eur. Polym. J.* **2007**, *43*, 2594.
(9) Platz, M. S. *Photochem. Photobiol.* **1997**, *65*, 193.
(10) Iwamura, H. *Pure Appl. Chem.* **1987**, *59*, 1595.
(11) Singh, P. N. D.; Mandel, S. M.; Sankaranarayanan, J.; Muthukrishnan, S.; Chang, M.; Robinson, R. M.; Lahti, P. M.; Ault, B. S.; Gudmundsdottir, A. D. *J. Am. Chem. Soc.* **2007**, *129*, 16263.
(12) Sankaranarayanan, J.; Rajam, S.; Hadad, C. M.; Gudmundsdottir, A. D. *J. Phys. Org. Chem.* **2010**, *23*, 370.
(13) Sankaranarayanan, J.; Bort, L. N.; Mandel, S. M.; Chen, P.; Krause, J. A.; Brooks, E. E.; Tsang, P.; Gudmundsdottir, A. D. *Org. Lett.* **2008**, *10*, 937.
(14) Muthukrishnan, S.; Ranaweera, R. A. A. U.; Gudmundsdottir, A. D. In *Nitrenes and Nitrenium Ions*; Falvey, D. E., Gudmundsdottir, A. D., Eds.; John Wiley & Sons: Hoboken, NJ, 2013; Vol. 6.
(15) Liang, T. Y.; Schuster, G. B. *J. Am. Chem. Soc.* **1987**, *109*, 7803.
(16) Pritchina, E. A.; Gritsan, N. P. *J. Photochem. Photobiol., A* **1988**, *43*, 165.
(17) Gritsan, N. P.; Pritchina, E. S. *J. Inf. Rec. Mater.* **1989**, *17*, 391.
(18) Rajam, S.; Murthy, R. S.; Jadhav, A. V.; Li, Q.; Keller, C.; Carra, C.; Pace, T. C. S.; Bohne, C.; Ault, B. S.; Gudmundsdottir, A. D. *J. Org. Chem.* **2011**, *76*, 9934.
(19) Inui, H.; Murata, S. *J. Am. Chem. Soc.* **2005**, *127*, 2628.
(20) Singh, B.; Zweig, A.; Gallivan, J. B. *J. Am. Chem. Soc.* **1972**, *94*, 1199.
(21) Barcus, R. L.; Hadel, L. M.; Johnston, L. J.; Platz, M. S.; Savino, T. G.; Scaiano, J. C. *J. Am. Chem. Soc.* **1986**, *108*, 3928.
(22) Mueller, F.; Mattay, J.; Steenken, S. *J. Org. Chem.* **1993**, *58*, 4462.
(23) Orton, E.; Collins, S. T.; Pimentel, G. C. *J. Phys. Chem.* **1986**, *90*, 6139.
(24) Barcus, R. L.; Wright, B. B.; Platz, M. S.; Scaiano, J. C. *Tetrahedron Lett.* **1983**, *24*, 3955.
(25) Padwa, A.; Rosenthal, R. J.; Dent, W.; Filho, P.; Turro, N. J.; Hrovat, D. A.; Gould, I. R. *J. Org. Chem.* **1984**, *49*, 3174.
(26) Bornemann, C.; Klessinger, M. *Chem. Phys.* **2000**, *259*, 263.
(27) Lee, C.; Yang, W.; Parr, R. G. *Phys. Rev. B: Condens. Matter* **1988**, *37*, 785.
(28) Frisch, M. J.; et al. *Gaussian*, 03; Gaussian: Wallingford CT, 2004.
(29) Becke, A. D. *J. Chem. Phys.* **1993**, *98*, 5648.
(30) Muthukrishnan, S.; Mandel, S. M.; Hackett, J. C.; Singh, P. N. D.; Hadad, C. M.; Krause, J. A.; Gudmundsdottir, A. D. *J. Org. Chem.* **2007**, *72*, 2757.
(31) Muthukrishnan, S.; Sankaranarayanan, J.; Klima, R. F.; Pace, T. C. S.; Bohne, C.; Gudmundsdottir, A. D. *Org. Lett.* **2009**, *11*, 2345.
(32) Clark, W. D. K.; Steel, C. *J. Am. Chem. Soc.* **1971**, *93*, 6347.
(33) Upul Ranaweera, R. A. A.; Sankaranarayanan, J.; Casey, L.; Ault, B. S.; Gudmundsdottir, A. D. *J. Org. Chem.* **2011**, *76*, 8177.
(34) Muthukrishnan, S.; Sankaranarayanan, J.; Pace, T. C. S.; Konosonoks, A.; DeMichiei, M. E.; Meese, M. J.; Bohne, C.; Gudmundsdottir, A. D. *J. Org. Chem.* **2010**, *75*, 1393.
(35) Rajam, S.; Murthy, R. S.; Jadhav, A. V.; Li, Q.; Keller, C.; Carra, C.; Pace, T. C. S.; Bohne, C.; Ault, B. S.; Gudmundsdottir, A. D. *J. Org. Chem.* **2011**, *76*, 9934.
(36) Albrecht, E.; Mattay, J.; Steenken, S. *J. Am. Chem. Soc.* **1997**, *119*, 11605.
(37) Nunes, C. M.; Reva, I.; Pinho e Melo, T. M. V. D.; Fausto, R.; Šolomek, T.; Bally, T. *J. Am. Chem. Soc.* **2011**, *133*, 18911.
(38) Wenthold, P. G. *J. Org. Chem.* **2012**, *77*, 208.
(39) Lee, C.; Yang, W.; Parr, R. G. *Phys. Rev. B: Condens. Matter* **1988**, *37*, 785.
(40) Gonzalez, C.; Schlegel, H. B. *J. Chem. Phys.* **1989**, *90*, 2154.
(41) Gonzalez, C.; Schlegel, H. B. *J. Phys. Chem.* **1990**, *94*, 5523.
(42) Labanowksi, J. K., Andzelm, J. W., Eds. *Density Functional Methods in Chemistry*; Springer-Verlag: New York, Weinheim, 1991.
(43) Bauernschmitt, R.; Ahlrichs, R. *Chem. Phys. Lett.* **1996**, *256*, 454.
(44) Foresman, J. B.; Head-Gordon, M.; Pople, J. A.; Frisch, M. J. *J. Phys. Chem.* **1992**, *96*, 135.
(45) Stratmann, R. E.; Scuseria, G. E.; Frisch, M. J. *J. Chem. Phys.* **1998**, *109*, 8218.
(46) Cances, E.; Mennucci, B. *J. Chem. Phys.* **2001**, *114*, 4744.
(47) Cramer, C. J.; Truhlar, D. G. *Chem. Rev.* **1999**, *99*, 2161.
(48) Mennucci, B.; Cances, E.; Tomasi, J. *J. Phys. Chem. B* **1997**, *101*, 10506.
(49) Tomasi, J.; Mennucci, B.; Cammi, R. *Chem Rev* **2005**, *105*, 2999.
(50) Renfrow, W. B.; Witte, J. F.; Wolf, R. A.; Bohl, W. R. *J. Org. Chem.* **1968**, *33*, 150.